

NASA TECHNICAL NOTE



NASA TN D-5604

c. 1

NASA TN D-5604



LOAN COPY: RETURN TO
AFWL (WLOL)
KIRTLAND AFB, N MEX

TURBINE PERFORMANCE IN A GAS-BEARING BRAYTON CYCLE TURBOALTERNATOR

by Joseph S. Curreri, Roman Kruchowy, and James C. Wood

Lewis Research Center

Cleveland, Ohio

NATIONAL AERONAUTICS AND SPACE ADMINISTRATION • WASHINGTON, D. C. • DECEMBER 1969



0132571

1. Report No. NASA TN D-5604	2. Government Accession No.	3. Recipient's Catalog No.	
4. Title and Subtitle TURBINE PERFORMANCE IN A GAS-BEARING BRAYTON CYCLE TURBOALTERNATOR		5. Report Date December 1969	6. Performing Organization Code
7. Author(s) Joseph S. Curreri, Roman Kruchowy, and James C. Wood		8. Performing Organization Report No. E-5314	
9. Performing Organization Name and Address Lewis Research Center National Aeronautics and Space Administration Cleveland, Ohio 44135		10. Work Unit No. 120-27	11. Contract or Grant No.
12. Sponsoring Agency Name and Address National Aeronautics and Space Administration Washington, D. C. 20546		13. Type of Report and Period Covered Technical Note	
15. Supplementary Notes			
16. Abstract The performance characteristics of the turbine for a gas-bearing Brayton cycle turboalternator were experimentally determined and compared with design predictions. Design operating conditions were inlet temperature, 1225 ^o F (936 K); inlet pressure, 8.45 psia (5.83 N/cm ² abs); total- to static-pressure ratio, 1.26; and shaft speed, 12 000 rpm. Performance data were obtained over a range of pressure ratios from 1.1 to 1.4 and at speeds of 10 000, 12 000, and 14 400 rpm.			
17. Key Words (Suggested by Author(s)) Gas-bearing turboalternator Brayton cycle energy conversion		18. Distribution Statement Unclassified - unlimited	
19. Security Classif. (of this report) Unclassified	20. Security Classif. (of this page) Unclassified	21. No. of Pages 16	22. Price* \$3.00

*For sale by the Clearinghouse for Federal Scientific and Technical Information
Springfield, Virginia 22151

TURBINE PERFORMANCE IN A GAS-BEARING BRAYTON CYCLE TURBOALTERNATOR

by Joseph S. Curreri, Roman Kruchowy, and James C. Wood

Lewis Research Center

SUMMARY

Performance of the turbine for a gas-bearing Brayton cycle turboalternator was determined from the turboalternator test. The design operating conditions were turbine inlet temperature, 1225^o F (936 K); turbine inlet pressure, 8.45 psia (5.83 N/cm² abs); total- to static-pressure ratio, 1.26; and shaft speed, 12 000 rpm. Performance data were obtained over a range of pressure ratios from 1.1 to 1.4 and at speeds of 10 000, 12 000, and 14 400 rpm.

The results of the investigation showed that, at the design speed and pressure ratio, the equivalent mass flow rate was 1.55 pounds per second (0.71 kg/sec), and the corresponding equivalent torque was 100 pound-inches (11.3 N-m). The overall total and static efficiencies of the turboalternator were 0.72 and 0.71, respectively. The total and static efficiencies of the turbine were 0.79 and 0.78, respectively. The turbine performance agreed with the results obtained from previous cold-component tests on an identical turbine.

INTRODUCTION

The NASA Lewis Research Center is presently investigating nuclear and solar dynamic power conversion systems for space flight application. One such system operating on the Brayton thermodynamic cycle and using argon as the working fluid is described in reference 1. One of the major components under investigation in this system is a turbine-driven alternator. This gas-bearing turboalternator was designed and built under contract to NASA. The alternator was designed for a 12-kilowatt output at a frequency of 400 hertz. The two-stage axial-flow turbine was designed to use argon at an inlet pressure and temperature of 8.45 psia (5.83 N/cm² abs) and 1225^o F (936 K), respectively, and was designed to run at a rotational speed of 12 000 rpm. The design inlet-total- to exit-static-pressure ratio was 1.26. At these conditions, the turboalternator output was 9 kilowatts.

Design information separately describing the turbine, the alternator, and the gas bearings can be found in references 2 to 7. Cold-gas component tests of the turbine at two values of rotor-blade-tip clearance are discussed in references 8 and 9; these cold-gas component tests were conducted at a turbine inlet temperature of 150°F (339 K).

The hot-gas operating characteristics (evaluated at design conditions) of the turboalternator with gas bearings are discussed in a preliminary nature in reference 10. The hot-gas performance of the gas bearings is discussed in detail in references 11 and 12.

This report presents an experimental evaluation of the turboalternator with the turbine having a rotor-blade-tip clearance (radial) of 0.031 inch (0.079 cm). Performance tests were made with argon at the design inlet temperature and pressure, over a range of total- to static-pressure ratios from 1.1 to 1.4, and at speeds of 10 000, 12 000, and 14 400 rpm. Data are presented to show the overall performance of both the turbine and the turboalternator. The results are expressed in terms of equivalent mass flow rate, equivalent torque, efficiency, and alternator output power. The results are compared with the design predictions and with the cold-gas performance of reference 9.

SYMBOLS

C	bearing clearance, in.; cm
c_p	specific heat at constant pressure, Btu/lb; J/kg
D	journal diameter, in.; cm
e	eccentricity ratio, e_B/c
e_B	bearing eccentricity, distance between bearing and journal centers, in.; cm
H	bearing friction loss, W
L	journal length, in.; cm
P	absolute pressure, psia; N/cm^2 abs
P_a	ambient pressure of thrust bearing cavity, psia; N/cm^2 abs
P_R	pressure ratio
$P_{wr, out}$	alternator output power, W
R_i	inside radius of thrust bearing, in.; cm
R_o	outside radius of thrust bearing, in.; cm

T	absolute temperature at turbine inlet, °R; K
U_m	blade velocity at mean rotor blade section, ft/sec; m/sec
V	absolute gas velocity, ft/sec; m/sec
V_j	isentropic jet speed corresponding to total- to static-pressure ratio across turbine
w	turbine weight flow, lb/sec; kg/sec
Γ	thrust bearing torque, lb-in.; N-m
Γ_u	thrust bearing unit torque
γ	ratio of specific heats
δ	ratio of inlet total pressure to U. S. standard sea-level pressure
ϵ	function of γ used in relating parameters to those using air inlet conditions at U. S. standard sea-level conditions, $\frac{0.740(\gamma + 1)}{\gamma} \left(\frac{\gamma + 1}{2} \right)^{\gamma/(\gamma-1)}$
η_{alt}	alternator efficiency
η_{tas}	static efficiency of turboalternator
η_{tat}	total efficiency of turboalternator
η_{ts}	static efficiency of turbine
η_{tt}	total efficiency of turbine
θ_{cr}	squared ratio of critical velocity at turbine inlet to critical velocity at U. S. standard sea-level temperature, $(V_{cr}/V_{cr}^*)^2$
Λ_c	compression number
μ	viscosity, (lb)(sec)/in. ² ; (N)(sec)/cm ²
ν	blade-jet speed ratio, U_m/V_j
τ	turbine torque, in.-lb; N-m
ω	shaft rotational speed, rad/sec

Subscripts:

cr	condition corresponding to Mach 1
JB1	drive end journal bearing
JB2	antidrive end journal bearing
T	thrust bearing

- 1 station at turbine inlet
- 2 station at turbine outlet

Subscripts:

- ' total state
- * U. S. standard sea-level conditions; temperature, 518.67° R (288.15 K); pressure, 14.696 psia (10.133 N/cm² abs)

APPARATUS AND PROCEDURE

Turboalternator

The gas-bearing turboalternator consisted of a two-stage axial-flow turbine and a 12-kilowatt four-pole homopolar inductor alternator. The design shaft rotational speed was 12 000 rpm. A cross-sectional view of the turboalternator is shown in figure 1.

The shaft was supported by two self-acting tilting-pad journal bearings (four 80° partial-arc pads per bearing) and an inward-pumping spiral-grooved self-acting thrust bearing. Details of the gas-bearing system are presented in reference 3.

The internal operating temperatures of the turboalternator were maintained by two coolant systems: (1) coolant oil that flowed through the alternator stator and heat exchangers of each of the bearings and (2) externally supplied cooling argon that flowed from the thrust bearing end through and around the hollow shaft, through the bearing cavities of each bearing, and then into the main gas stream at the turbine seals. The cooling argon flow rate was about 0.5 percent of the main gas flow rate.

Test Facility

The Brayton cycle turboalternator test facility is described in detail in reference 10. A simplified schematic flow diagram of the facility is shown in figure 2.

Recirculating argon was heated by the electric heater. Turbine inlet pressure was controlled by regulating the flow through the turbine bypass line. The pressure ratio across the turbine was controlled by the valve at the turbine discharge. This valve was also used to control speed. The electrical output of the alternator was absorbed by resistive load banks.

The coolant loop supplied coolant to the alternator stator and to the heat exchangers of each of the bearings. Coolant flow rate and temperature to each of these components could be controlled individually.

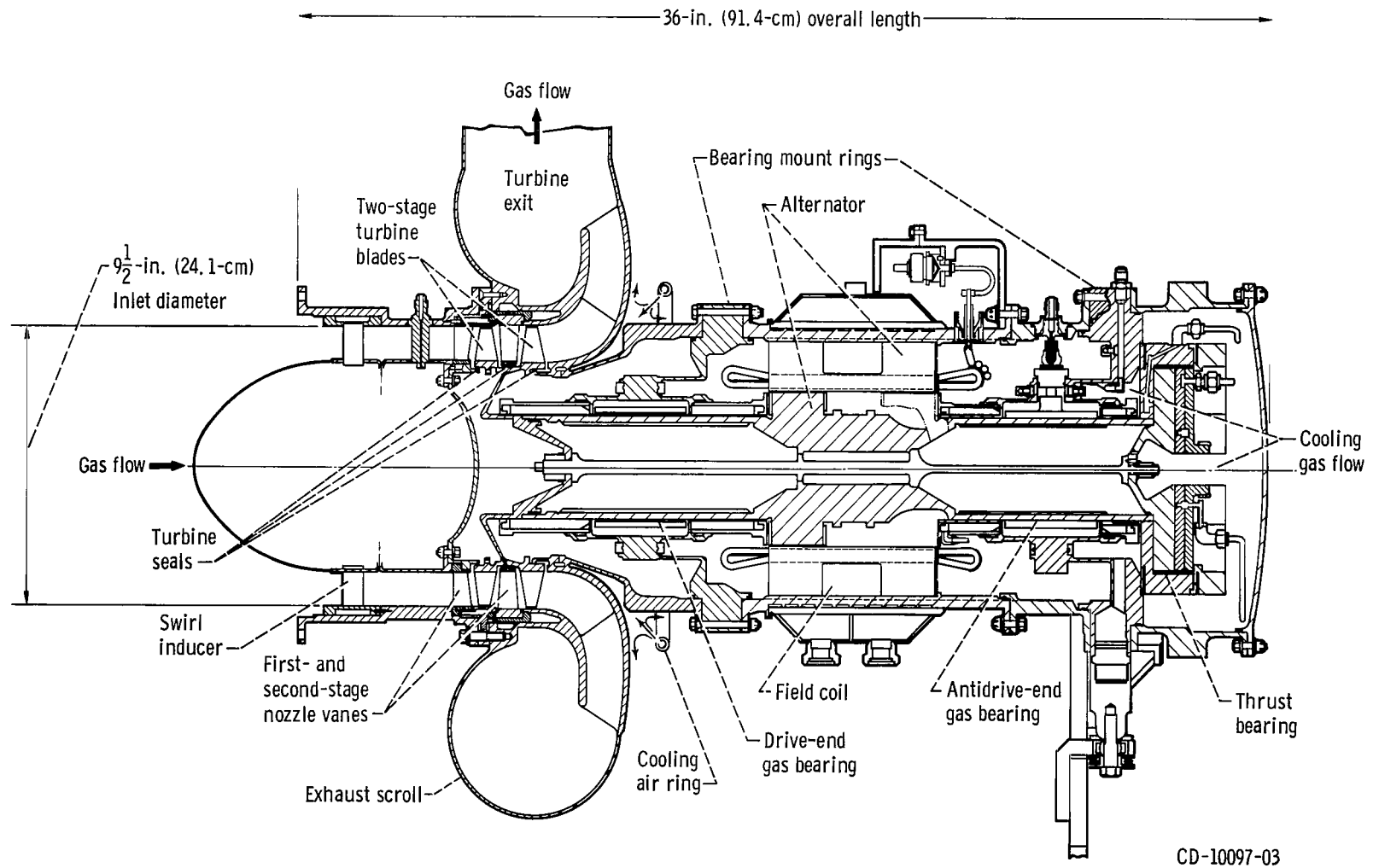


Figure 1. - Cross-sectional view of turboalternator.

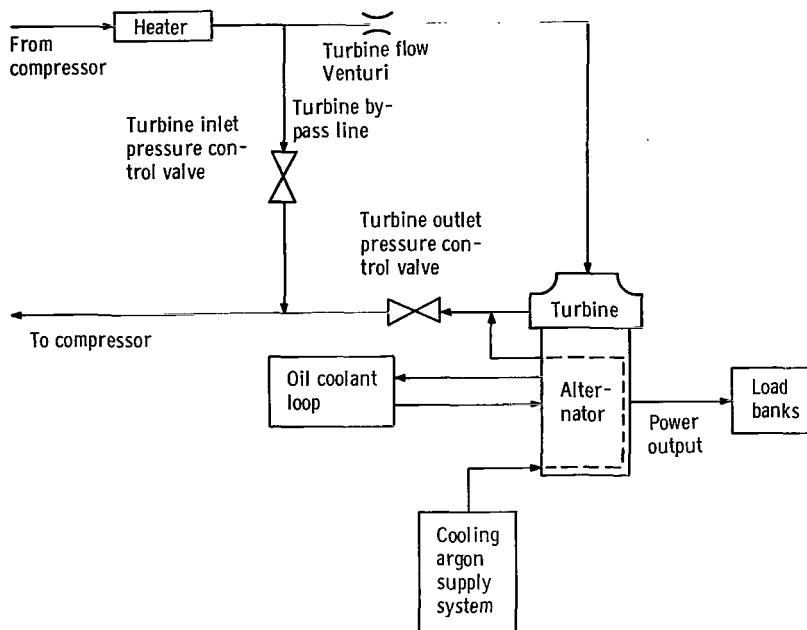


Figure 2. - Brayton cycle turboalternator test facility.

Instrumentation

Chromel-Alumel thermocouples were used to measure turboalternator internal temperatures and turbine inlet and outlet gas temperatures. The inlet and outlet gas temperatures were measured with bare-spike thermocouples mounted on rakes. The oil coolant temperatures were measured with iron-constantan thermocouples immersed in the oil stream.

Turboalternator case pressures and static and total pressures at the turbine inlet and outlet were measured with a strain-gage-type pressure transducer.

Turbine weight flow was measured with a calibrated Venturi meter located upstream of the turbine. Liquid coolant flow rates were measured with turbine flowmeters and gas coolant flow rates with rotameters. The clearance of the bearings was measured with capacitance-type distance probes.

Alternator output was measured with instruments of the wide-frequency-range true-rms electronic type. Turboalternator shaft speed was measured with three magnetic speed pickups and a digital counter.

Operating Procedure

The tests were conducted by holding turbine speed and inlet pressure constant and

varying pressure ratio (exhaust pressure). By manually setting alternator load, the speed control would automatically adjust pressure ratio to maintain constant speed.

METHOD OF ANALYSIS

Turbine performance was determined from the overall turboalternator performance by allowing for alternator, bearing, and windage losses. Turbine power could not be measured directly because of high heat loss from the turbine. Cooling air was blown over the forward bearing mount ring (fig. 1) to protect the bearing instrumentation from over temperature. The cooling air lowered the temperature of the mount ring, as intended, but it also cooled the turbine exhaust scroll. Because of the scroll heat loss, the exhaust gas temperatures could not be used to evaluate turbine performance. Exhaust gas pressures were not affected by the lower exhaust gas temperatures.

The overall efficiency of the turboalternator was determined from the measured alternator output power $P_{wr, out}$ and the turbine isentropic input power. The turbine input power was computed from the measured values of weight flow w , turbine inlet absolute temperature T , and turbine pressure ratio P_R :

$$\text{Overall efficiency} = \frac{\text{measured alternator output power}}{\text{turbine isentropic input power}} \quad (1)$$

where

$$\text{Turbine isentropic input power} = wc_p T \left[1 - (P_R)^{(\gamma-1)/\gamma} \right] \quad (2)$$

The overall turboalternator static efficiency η_{tas} was based on turbine-outlet-static-to inlet-total-pressure ratio $P_R = P_2/P_1'$, and the overall turboalternator total efficiency η_{tat} was based on turbine-outlet-total- to inlet-total-pressure ratio $P_R = P_2^v/P_1'$, or, respectively,

$$\eta_{tas} = \frac{P_{wr, out}}{wc_p T \left[1 - \left(\frac{P_2}{P_1'} \right)^{(\gamma-1)/\gamma} \right]} \quad (3)$$

and

$$\eta_{tat} = \frac{P_{wr, out}}{wc_p T \left[1 - \left(\frac{P_2'}{P_1'} \right)^{(\gamma-1)/\gamma} \right]} \quad (4)$$

The turbine static efficiency η_{ts} and total efficiency η_{tt} were obtained as follows:

$$\eta_{ts} = \frac{\frac{P_{wr, out}}{wc_p T} + H}{\eta_{alt} \left[1 - \left(\frac{P_2'}{P_1'} \right)^{(\gamma-1)/\gamma} \right]} \quad (5)$$

$$\eta_{tt} = \frac{\frac{P_{wr, out}}{wc_p T} + H}{\eta_{alt} \left[1 - \left(\frac{P_2'}{P_1'} \right)^{(\gamma-1)/\gamma} \right]} \quad (6)$$

where η_{alt} is the alternator efficiency and H is the total bearing friction power loss. The alternator efficiencies were obtained from the curve of alternator efficiency against alternator output power presented in the alternator performance tests of reference 7. The alternator efficiency presented in reference 7 includes all alternator losses but does not include bearing losses.

The bearing friction power loss term H used in equations (5) and (6) includes the losses of the thrust bearing H_T and both journal bearings H_{JB1} and H_{JB2} . Details of bearing geometries can be found in reference 3. The equations used to solve for thrust bearing losses can be found in reference 13.

The following thrust bearing power loss equations were used:

$$H_T = \Gamma \omega \quad (7)$$

where

$$\Gamma = \frac{\pi P_a C}{6} (R_o^2 + R_i^2) \Lambda_c \Gamma_u \quad (8)$$

and

$$\Lambda_c = \frac{3\mu W (R_o^2 - R_i^2)}{P_a C^2} \quad (9)$$

where Γ_u is found from figure 6.3.14 of reference 13.

The friction power dissipated in each journal bearing was calculated by

$$H_{JB} = \frac{4 \times 80^0}{360^0} \left(\frac{\pi \mu \omega^2 L D^3}{4C \sqrt{1 - e^2}} \right) \quad (10)$$

An eccentricity ratio e of 0.7 was used (ref. 3).

RESULTS AND DISCUSSION

The variation of equivalent mass flow rate with outlet-static- to inlet-total-air equivalent pressure ratio for lines of constant speed is shown in figure 3. The curves are typical of subsonic turbines. At the design equivalent outlet- to inlet-pressure ratio and speed (0.809 and 12 000 rpm, respectively), the mass flow rate was 1.55 pounds per second (0.71 kg/sec). This flow rate is less than 1 percent higher than the design prediction of 1.54 pounds per second (0.70 kg/sec) and is approximately 3 percent higher

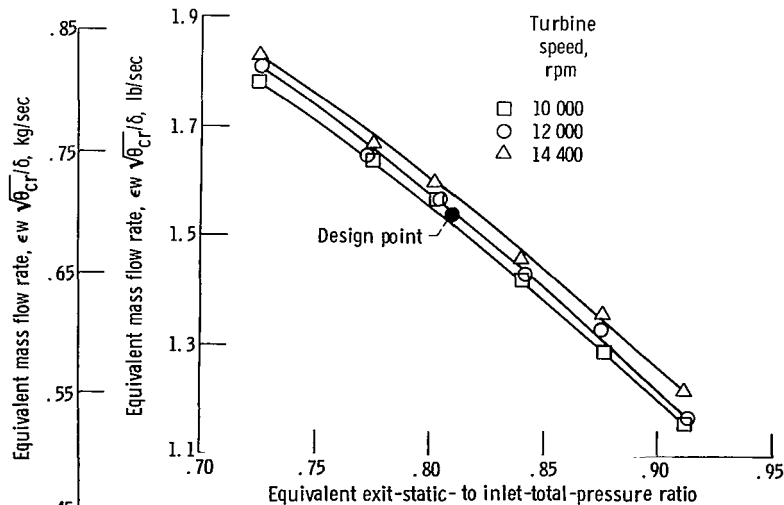


Figure 3. - Variation of equivalent mass flow rate with pressure ratio.

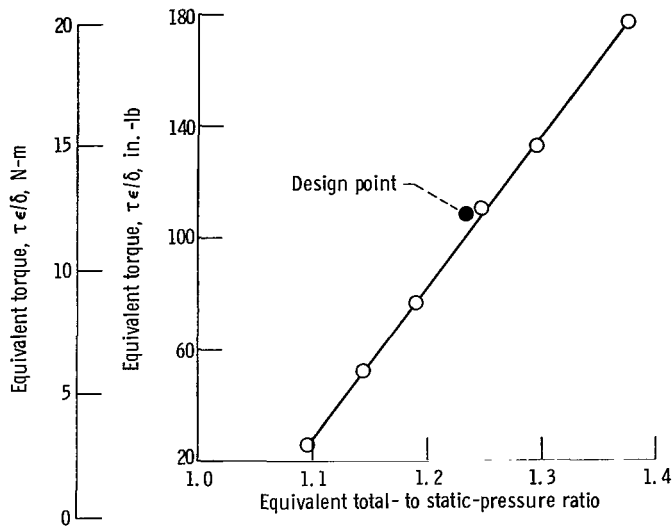


Figure 4. - Variation of equivalent torque with equivalent pressure ratio at 12 000 rpm.

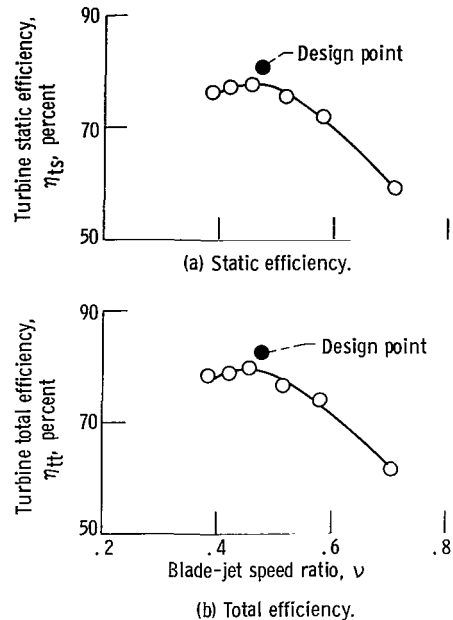


Figure 5. - Variation of turbine efficiency with blade-jet speed ratio at 12 000 rpm.

than the results obtained from the cold-component test on an identical turbine (ref. 9).

The variation of equivalent torque $\tau\epsilon/\delta$ with equivalent total- to static-pressure ratio at design speed is shown in figure 4. The curve indicates that at the design equivalent pressure ratio (1.23) the equivalent torque is 100 pound-inches (11.3 N-m). This torque value is approximately 8 percent lower than the design prediction of 108 pound-inches (12.2 N-m) and is identical to the torque value obtained in reference 9.

The variation of static and total turbine efficiency with blade-jet speed ratio is shown in figures 5(a) and (b), respectively. At design conditions, the turbine static and total efficiencies are 0.78 and 0.79, respectively. The efficiencies are approximately 5 percentage points lower than the design predictions and within 1 percentage point of the results obtained in reference 9. At peak efficiency, the blade-jet speed ratio was 0.455.

The variation of overall turboalternator efficiency with alternator output power for three values of shaft speed is shown in figure 6. The curves represent the static and total efficiencies of the entire turbine-alternator package. The results include the combined efficiencies of the turbine and the alternator, as well as the bearing losses. At the design speed and pressure ratio, the overall static efficiency was 0.71, and the overall total efficiency was 0.72.

The calculated thrust and journal bearing friction power losses as a function of their measured clearances are shown in figures 7 and 8, respectively, for speeds from

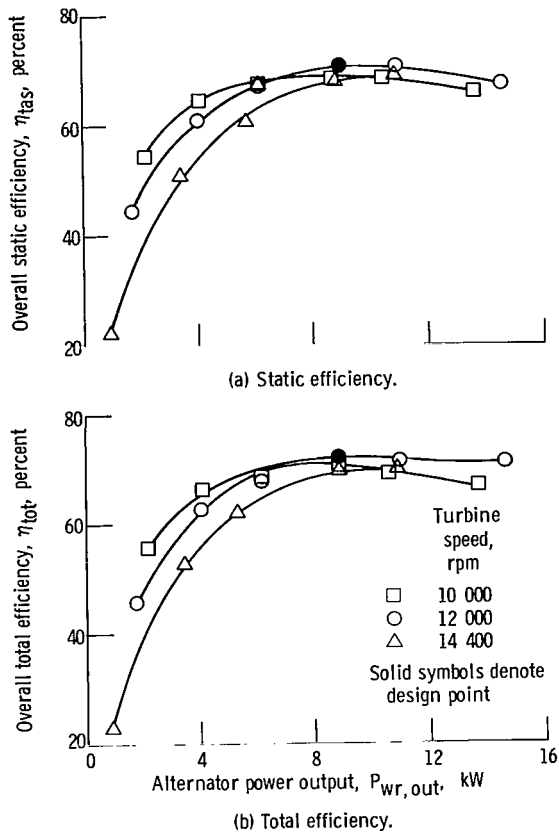


Figure 6. - Variation of overall turboalternator efficiency with alternator output power.

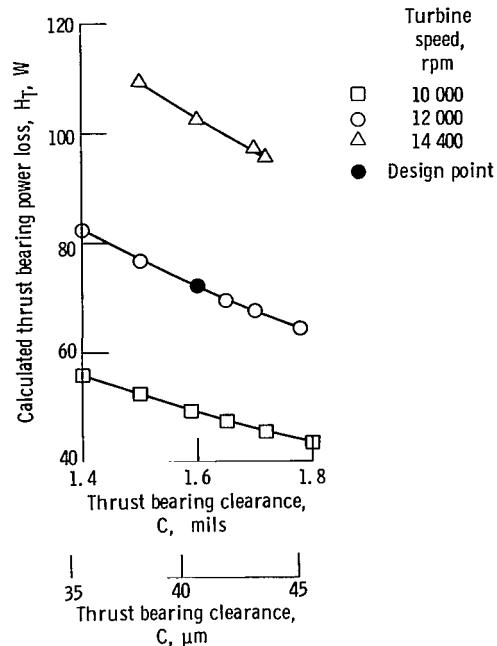


Figure 7. - Variation of computed thrust bearing friction power loss with clearance.

10 000 to 14 400 rpm. The data were computed using equations (7) to (10). At the design speed and pressure ratio, the calculated bearing friction power dissipated was 72.2 watts for the thrust bearing at a clearance of 1.6 mils (41 μm), 106 watts for the drive-end journal bearing at a clearance of 1.02 mils (26 μm), and 111 watts for the antidrive-end journal bearing at a clearance of 0.945 mil (24 μm).

A breakdown of the energy input to the turboalternator is presented in figure 9. The results are presented in terms of alternator output power, alternator input power, turbine output power, and turbine isentropic input power as a function of turbine total- to static-pressure ratio. The results were obtained at the turbine design speed of 12 000 rpm and inlet temperature of 1225^o F (936 K). Alternator losses are represented by the difference between the alternator input and output curves; bearing losses are represented by the difference between the turbine output and alternator input curves; turbine aerodynamic losses are represented by the difference between the turbine isentropic total input and turbine output power curves; and the kinetic energy in the exhaust gas is represented by the difference between the turbine isentropic static and total input power curves.

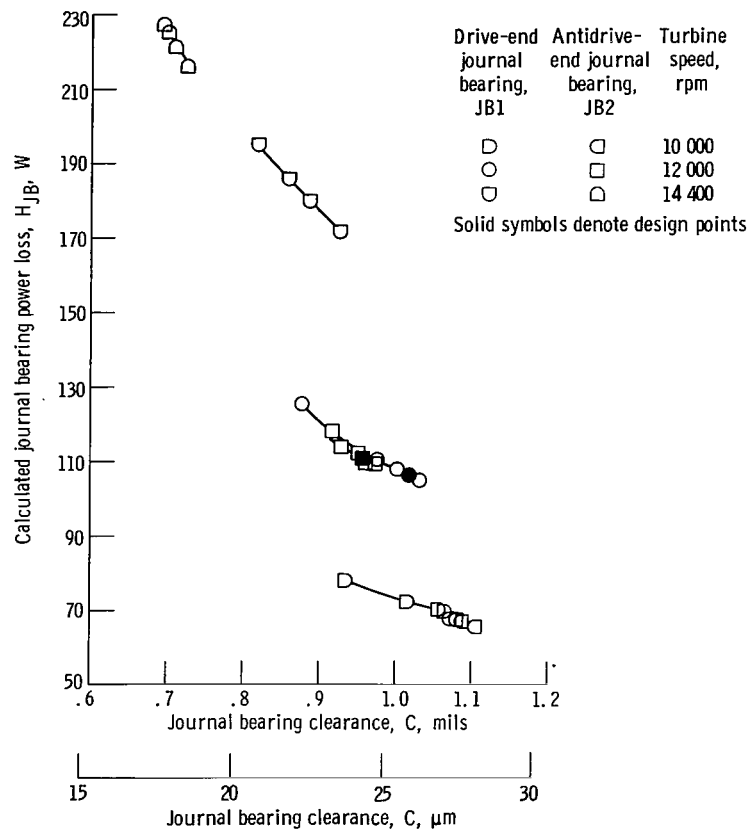


Figure 8. - Variation of computed journal bearing friction power loss with clearance.

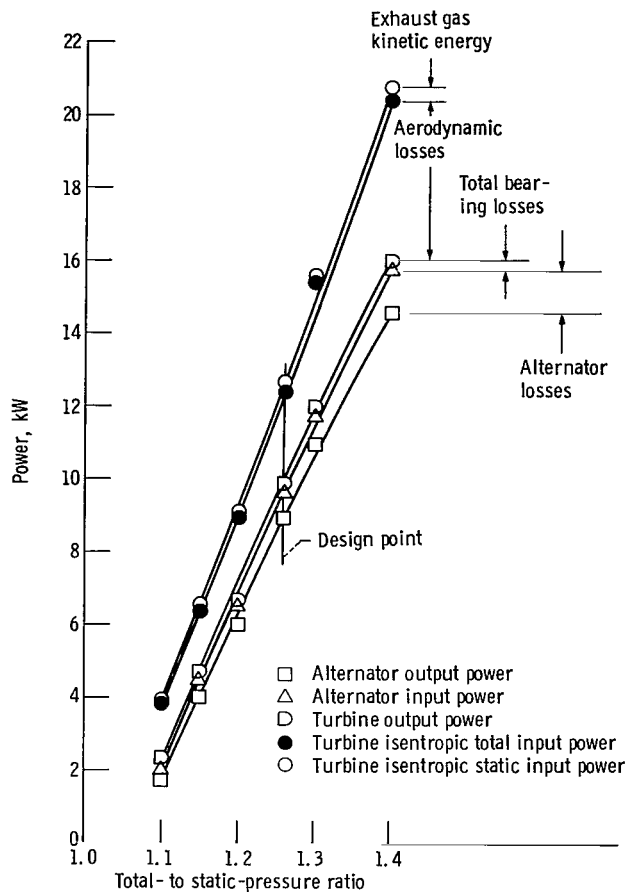


Figure 9. - Breakdown of energy input to turboalternator for various pressure ratios at turbine design speed and inlet temperature.

SUMMARY OF RESULTS

For a 9-kilowatt turbine-driven alternator supported by gas-lubricated bearings, turbine operating characteristics were obtained from the overall turboalternator performance. The results of the investigation are summarized as follows:

1. At design speed and equivalent pressure ratio, the equivalent mass flow rate was 1.55 pounds per second (0.71 kg/sec). This value is less than 1 percent higher than the design prediction and approximately 3 percent higher than that obtained from the cold-component test on an identical turbine.

2. The corresponding equivalent torque was 100 pound-inches (11.3 N-m), which is identical to the results obtained in the cold-component test and is 8 percent less than the design prediction of 108 pound-inches (12.2 N-m).

3. The overall total and static efficiencies of the turboalternator were 0.72 and 0.71, respectively, at design turbine conditions.

4. The total and static efficiencies of the turbine were 0.79 and 0.78, respectively, at design conditions. These efficiencies are within 1 percent of those obtained in the cold-component test and are approximately 5 percentage points lower than the design prediction.

Lewis Research Center,
National Aeronautics and Space Administration,
Cleveland, Ohio, October 9, 1969,
120-27.

REFERENCES

1. Bernatowicz, Daniel T.: NASA Solar Brayton Cycle Studies. Paper presented at the Symposium on Solar Dynamics Systems, Interagency Advanced Power Group, Washington, D.C., Sept. 24-25, 1963.
2. Cohen, R.; Gilroy, W. K.; and Spencer, W. B.: High-Performance Turboalternator and Associated Hardware. I - Design of Turboalternator. NASA CR-1290, 1969.
3. Frost, A.; Lund, J. W.; and Curwen, P. W.: High-Performance Turboalternator and Associated Hardware. II - Design of Gas Bearings. NASA CR-1291, 1969.
4. Cohen, R.; Gilroy, W. K.; and Havens, F. D.: Turbine Research Package for Research and Development of High Performance Turboalternator. Rep. PWA-2796, Pratt & Whitney Aircraft (NASA CR-54885), Jan. 1967.
5. Dryer, A. M. et al.: Alternator and Voltage Regulator-Exciter for a Brayton Cycle Space Power System. Vol. I - Alternator and Voltage Regulator-Exciter Design and Development. Rep. GE-A69-003, General Electric Co., May 1969. (Work done under contract NAS3-6013.)
6. Greenwell, J. E.; Russell, E. F.; and Yeager, L. J.: Alternator and Voltage Regulator-Exciter for a Brayton Cycle Space Power System. Vol. II - Unbalanced Electromagnetic Forces Investigation. Rep. GE-A69-003, General Electric Co., May 1969. (Work done under contract NAS3-6013.)
7. Edkin, Richard A.; Valgora, Martin E.; and Perz, Dennis A.: Performance Characteristics of a 15 kVA Homopolar Inductor Alternator for 400 Hz Brayton-Cycle Space-Power System. NASA TN D-4698, 1968.
8. Kofskey, Milton G.; and Nusbaum, William J.: Aerodynamic Evaluation of Two-Stage Axial-Flow Turbine Designed for Brayton-Cycle Space Power System. NASA TN D-4382, 1968.

9. Kofskey, Milton G.; and Nusbaum, William J.: Performance Evaluation of a Two-Stage Axial-Flow Turbine for Two Values of Tip Clearance. NASA TN D-4388, 1968.
10. Wood, James C. et al.: Preliminary Performance Characteristics of a Gas-Bearing Turboalternator. NASA TM X-1820, 1969.
11. Kruchowy, R.; Wood, J. C.; and Curreri, J. S.: Performance of a Turbo-Alternator Gas-Bearing System at Steady-State Conditions. NASA TN D-5542, 1969.
12. Wood, James C.; Valgora, Martin, E.; and Tryon, H. B.: Hot Performance Characteristics of a Gas Bearing Brayton Cycle Turboalternator. Presented at the AIChE Fourth Intersociety Energy Conversion Engineering Conference, Washington, D.C., Sept. 21-26, 1969.
13. Anon.: Design of Gas Bearings. Vol. II - Notes Supplemental to the RPI-MTI Course on Gas Bearing Design. Mechanical Technology, Inc., 1967.
14. Bisson, Edmond E.; and Anderson, William J.: Advanced Bearing Technology. NASA SP-38, 1964.